JGR Atmospheres

RESEARCH ARTICLE
10.1029/2020JD033563

Special Section:
The Exceptional Arctic Polar Vortex in 2019/2020: Causes and Consequences

Exceptionally Low Arctic Stratospheric Ozone in Spring 2020 as Seen in the CAMS Reanalysis

A. Inness[1], S. Chabrillat[2], J. Flemming[1], V. Huijnen[3], B. Langenrock[2], J. Nicolas[1], I. Polichtchouk[1], and M. Razinger[1]

[1]ECMWF, Reading, UK, [2]Royal Belgian Institute for Space Aeronomy (BIRA-IASB), Brussels, Belgium, [3]Royal Netherlands Meteorological Institute, De Bilt, The Netherlands

Key Points:
- Arctic ozone columns in spring 2020 were the lowest since 1979 because the Arctic polar vortex was unusually strong, cold, and long lasting
- We see evidence of chlorine activation and the presence of polar stratospheric clouds over the Arctic in March 2020
- The CAMS reanalysis captures the 2020 Arctic stratospheric ozone well

Supporting Information:
- Supporting Information S1

Correspondence to:
A. Inness,
a.inness@ecmwf.int

Citation:
Inness, A., Chabrillat, S., Flemming, J., Huijnen, V., Langenrock, B., Nicolas, J., et al. (2020). Exceptionally low Arctic stratospheric ozone in spring 2020 as seen in the CAMS reanalysis. *Journal of Geophysical Research: Atmospheres*, *125*, e2020JD033563. https://doi.org/10.1029/2020JD033563

Received 22 JUL 2020
Accepted 23 OCT 2020
Accepted article online 3 NOV 2020

Abstract A reanalysis data set produced by the Copernicus Atmosphere Monitoring service (CAMS reanalysis, 2003 to present day) augmented by ERA5 data for the years before 2003 is used to describe the evolution of the 2020 Arctic ozone season and to compare it with years back to 1979. Ozone columns over large parts of the Arctic reached record low values in March and April 2020 because of an exceptionally strong, cold, and persistent Arctic polar vortex. Minimum ozone columns were below 250 DU for most of March and the first half of April, with the lowest values of 211 DU in the CAMS reanalysis found on 18 March. Such low values are extremely unusual for the Arctic. The previous years with similarly strong Arctic ozone depletion were 2011 and 1997 with minimum values of 232 and 217 DU, respectively. The performance of the CAMS ozone analysis is assessed by comparison with ozonesonde data and found to agree well with the independent observations. We find a clear sign of chemical ozone destruction with ozone severely depleted in a layer between 80 and 50 hPa in late March and early April when partial pressure values below 2 mPa were observed. Profiles from the limb sounders Atmospheric Chemistry Experiment-Fourier Transform Spectrometer (ACE-FTS) and Microwave Limb Sounder (MLS) show clear signs of chlorine activation and the presence of polar stratospheric clouds. Monthly mean ozone columns in March 2020 were up to 180 DU or 40% lower than the CAMS climatology (2003–2019) while values for 2011 and 1997 were lower by 31% and 35%, respectively.

Plain Language Summary The stratosphere is the layer of the atmosphere between about 15 and 50 km where most of the ozone resides. Usually, Arctic ozone reaches maximum values in the stratosphere during boreal spring. However, in spring 2020 the Arctic stratosphere was exceptionally cold, and ozone transport from the midlatitudes was inhibited. Because of the low temperatures, polar stratospheric clouds could form over the Arctic region and lead to stratospheric ozone destruction. This led to record low ozone columns in the Arctic at the end of March and the beginning of April 2020, with minimum values of 211 DU. This is lower than in 1997 and 2011, the previous two years that had exceptionally low ozone columns over the Arctic during spring. In spring 2020, the Arctic ozone layer showed clear signs of chemical ozone depletion with ozone almost completely destroyed in a layer around 18 km in a way that is usually only seen over the Antarctic during the austral spring, when the ozone hole forms.

1. Introduction

While we are used to ozone holes developing over the Antarctic every year during Austral spring (WMO [World Meteorological Organization], Scientific Assessment of Ozone Depletion, 2018), the conditions that are needed for such strong ozone depletion are normally not found in the Northern Hemisphere (NH). There, the wintertime polar vortex is usually weaker and more perturbed than in the Southern Hemisphere (SH), and stratospheric temperatures are not as low as over the Antarctic during austral winter and spring (Waugh et al., 2017). This is the result of greater planetary wave activity in the NH (Shepherd, 2008) because of the larger topographic and land-sea contrast than in the SH. These waves can propagate upward in the winter hemisphere when stratospheric winds are westerly and dissipate in the upper stratosphere ("wave breaking") decelerating the Arctic polar vortex and leading to a warmer and more perturbed Arctic stratosphere (Garcia & Boville, 1994). Because the Arctic polar vortex is less stable than the Antarctic one, more mixing occurs between the Arctic and ozone-richer midlatitudes than in the SH (Manney et al., 1994).

The wave drag also drives a poleward transport in the stratosphere from the ozone source regions in the tropics, with connected downward transport in the extratropics and upward transport in the tropics, as part of the large-scale overturning Brewer-Dobson circulation (Brewer, 1949; Dobson, 1956). Because the wave activity is stronger in the NH during winter/spring than in the SH, the Brewer-Dobson circulation is not symmetric in both hemispheres (Shepherd, 2008) but leads to a stronger buildup of ozone in the lower stratosphere at high northern latitudes during boreal spring than in the SH during austral spring. The downward transport at high latitudes also leads to adiabatic warming and overall higher temperatures in the lower stratosphere of the NH than the SH. Consequently, fewer polar stratospheric clouds (PSCs) form in the Arctic stratosphere during winter/spring, resulting generally in less severe catalytic ozone depletion than in the SH during austral winter/spring. Due to all these reasons, typical total column ozone (TCO3) values at the beginning of winter are naturally higher in the Arctic than in the Antarctic (Salawitch et al., 2019, Question 11). Consequently, even if severe chemical ozone depletion happened in the Arctic the resulting ozone columns would be larger than the very low values (below 100 DU) that were found in some years over the Antarctic (see NASA's Ozone Watch, https://ozonewatch.gsfc.nasa.gov/meteorology/annual_data.html). Manney et al. (2011) argue that ozone values below 250–275 DU in the Arctic during winter are exceptional and can be referred to as a NH ozone hole even though 220 DU is the usual SH ozone hole threshold.

Stratospheric ozone values over large parts of the Arctic reached record low values in March and April 2020 (Manney et al., 2020) with ozone severely depleted between mid-March and mid-April 2020 when ozonesondes observed minimum mixing ratios of 0.1–0.2 ppm around 17–19 km (Wohltmann et al., 2020), lower than observed in any previous year. Model simulations and evaluation against MLS data by Groß and Müller (2020) also confirmed these findings. The last time similarly low ozone columns were observed over the Arctic was during boreal spring 2011 (Manney et al., 2011) and 1997 (Newman et al., 1997). Lawrence et al. (2020) showed that the record breaking strong polar vortex in winter/spring 2020 developed as a combination of weak wave driving from the troposphere and a wave-reflecting configuration in the upper stratosphere. The 2020 Arctic polar vortex was cold enough to allow PSCs to form (Manney et al., 2020), leading to large stratospheric ozone losses.

The Copernicus Atmosphere Monitoring Service (CAMS, http://atmosphere.copernicus.eu), operated by the European Centre for Medium-Range Weather Forecasts (ECMWF) on behalf of the European Commission, provides daily analyses and 5-day forecasts of atmospheric composition, including analyses of stratospheric ozone in near real time (NRT). CAMS followed the evolution of the 2020 Arctic ozone depletion in NRT making use of the full three-dimensional ozone analysis fields to assess the evolution of the TCO3 field as well as the vertical structure of the ozone field. In addition to providing daily NRT analyses and forecasts, CAMS also produces a reanalysis of atmospheric composition (Inness et al., 2019), which covers the years from 2003 onward and again includes stratospheric ozone. This reanalysis uses a single version of the CAMS model and data assimilation system, taking care to minimize changes in the versions of the used emissions or assimilated satellite retrievals. It is now running close to NRT and allows us to intercompare recent years and to derive anomalies against climatologies calculated over the whole period of the CAMS reanalysis (2003–2019) while avoiding spurious effects from changes in the model and the assimilation system.

In this paper, we use ozone data from the CAMS reanalysis to document the evolution of the 2020 Arctic ozone field, as well as stratospheric temperatures and zonal winds, and compare stratospheric ozone during the Arctic winter and spring 2019/2020 with other years covered by the CAMS reanalysis. We use data from the ERA5 reanalysis (Hersbach et al., 2020) to extend the TCO3 time series back to 1979 and assess the performance of the CAMS reanalysis with ozonesondes and independent satellite retrievals.

The paper is structured in the following way. Section 2 describes the CAMS model and data assimilation system and gives some information about the quality of the CAMS ozone analysis fields. Section 3 looks at the Arctic stratospheric ozone field during the winter 2019/2020 and compares it with the seasons 2010/2011 and 1996/1997, and section 4 finishes with the conclusions.

2. Data Sets

2.1. The CAMS Model and Data Assimilation System

The chemical mechanism of ECMWF's Integrated Forecast System (IFS) is a modified and extended version of the Carbon Bond 2005 (CB05; Yarwood et al., 2005) chemical mechanism for the troposphere, as also

implemented in the chemical transport model (CTM) TM5 (Huijnen et al., 2010). CB05 is a tropospheric chemistry scheme with 55 species and 126 reactions. Stratospheric ozone chemistry in IFS (CB05) is parameterized by a linear ozone scheme (Cariolle & Déqué, 1986; Cariolle & Teyssèdre, 2007). This combination allows a realistic representation of tropospheric and stratospheric ozone concentrations (Huijnen et al., 2020; Inness et al., 2019). The chemistry module of the IFS together with its emissions is documented in more detail in Flemming et al. (2015) and Flemming et al. (2017) and the updates used in the CAMS reanalysis in Inness et al. (2019).

The IFS uses an incremental four-dimensional variational (4D-Var) data assimilation system (Courtier et al., 1994), and ozone is one of the atmospheric composition fields in the CAMS reanalysis that is included in the control vector and minimized together with the meteorological control variables. More details about the data assimilation system and background errors can be found in Inness et al. (2015) and Inness et al. (2019). Ozone retrievals from a range of satellites are assimilated in the CAMS reanalysis. These data include TCO3 retrievals from the SCanning Imaging Absorption spectroMeter for Atmospheric CHartographY (SCIAMACHY) instrument, the Ozone Monitoring Instrument (OMI), and the Global Ozone Monitoring Experiment-2 (GOME-2); ozone profile data from the Michelson Interferometer for Passive Atmospheric Sounding (MIPAS) and Microwave Limb Sounder (MLS); and partial ozone columns from Solar Backscatter ULTra-Violet (SBUV/2). More information about the assimilated ozone retrievals can be found in Inness et al. (2019). The data used in 2020 are OMI, GOME-2, MLS, and SBUV/2. Particularly important for a realistic vertical distribution of the ozone analysis in the CAMS system is the assimilation of profile retrievals from MIPAS and MLS (Flemming et al., 2011; Huijnen et al., 2020; Inness et al., 2013; Lefever et al., 2015) that give height resolved ozone information throughout the stratosphere, including data during the polar night.

Some validation of the CAMS reanalysis is given in Inness et al. (2019), and Huijnen et al. (2020) provide an evaluation of tropospheric ozone for the 2003–2016 time period. There are also extensive validation reports of the CAMS reanalysis available online (from https://atmosphere.copernicus.eu/eqa-reports-global-services). These studies show that stratospheric ozone in the CAMS reanalysis agrees to within $\pm$5–10% with ozonesondes and satellite observations and does not show any discernible trends in the bias. Additional targeted validation of the Arctic stratospheric ozone fields from the CAMS reanalysis for the period January 2003 to April 2020 against Fourier-Transform Infrared Spectroscopy (FTIR) observations from the Network for the Detection of Atmospheric Composition Change (NDACC) network and the limb scanning satellite instruments MLS (Livesey et al., 2018) and Atmospheric Chemistry Experiment-Fourier Transform Spectrometer (ACE-FTS; Sheese et al., 2017) and MIPAS (Laeng et al., 2018) is shown in the supporting information. It confirms that the CAMS reanalysis generally has a small negative bias (5–10%) for stratospheric ozone in the Arctic, often within the measurement uncertainties of the instruments. This gives us confidence that the CAMS reanalysis is a useful data set to study stratospheric ozone and will allow us to describe the evolution of Arctic stratospheric ozone field during the winter and spring of 2019/2020.

2.2. ERA5 Total Column Ozone Record

The CAMS reanalysis only goes back to 2003 because most of the atmospheric composition satellite retrievals became available with the launch of the Envisat and Aura satellites in 2002 and 2004, respectively. To extend the time series of Arctic TCO3 back in time, we use ozone columns from the ERA5 reanalysis (Hersbach et al., 2020) for the years 1979 to 2002. This reanalysis is also produced with the ECMWF IFS system, and while it does not include a comprehensive tropospheric chemistry, it uses the same stratospheric chemistry parameterization as the CAMS reanalysis. Therefore, stratospheric ozone or TCO3 can well be compared with the CAMS reanalysis data. In ERA5, ozone retrievals from GOME, GOME-2, MIPAS, MLS, OMI, SCIAMACHY, SBUV, and the Total Ozone Mapping Spectrometer (TOMS) are assimilated as well as ozone sensitive radiances from several infrared sounders: the High-resolution Infrared Radiation Sounder (HIRS), Atmospheric Infrared Sounder (AIRS), Infrared Atmospheric Sounding Interferometer (IASI), and Cross-track Infrared Sounder (CrIS); see Hersbach et al. (2020) for more details. The ozone sensitive radiances are not assimilated in the CAMS reanalysis. We restrict our use of ERA5 ozone data to TCO3 fields. These are usually well constrained by the assimilated satellite data, while vertical profiles may suffer from the lack of adequate ozone profile data during some of the years (Dragani, 2011; Hersbach et al., 2020). Hersbach et al. (2020) mention, for instance, that in the northern winter of 1996/1997, the ERA5 ozone

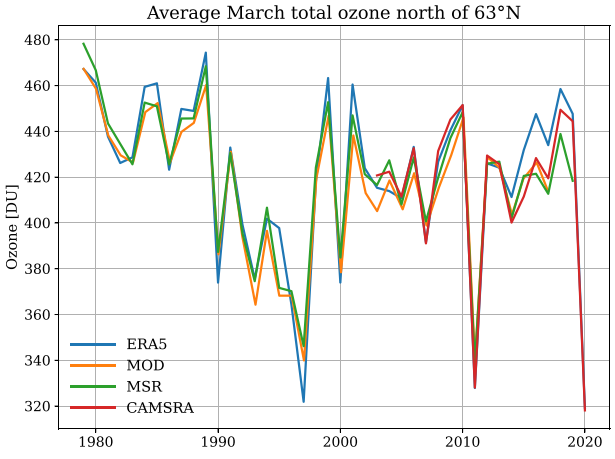

Figure 1. Time series of monthly mean March TCO3 in Dobson units (DU) averaged over the area north of 63°N from NASA's merged ozone data set (MOD, orange), ERA5 (blue), Multi Sensor Reanalysis (MSR, green), and CAMS reanalysis (CAMSRA, red).

values in the upper stratosphere at high northern latitudes are many times larger than normal but that this problem does not significantly affect total column ozone.

Figure 1 shows a time series of the monthly mean TCO3 values for March averaged over the area north of 63°N from the CAMS reanalysis, ERA5, the Multi Sensor Reanalysis (MSR) of total ozone (van der A et al., 2015) and NASA's Merged Ozone data set (MOD; Stolarski & Frith, 2006). It shows a good agreement between ERA5, MSR, and MOD data going back to 1979 with all data sets reproducing the interannual variability of TCO3 and agreeing to within 5%. ERA5 and CAMS reanalysis TCO3 values agree well for the years where the data sets overlap, but there is an increased discrepancy between ERA5 and the other data sets between 2014 and 2017. Such a positive anomaly was also noted by Hersbach et al. (2020) against a range of other reanalysis data sets and has now been traced back in part to a change from using reprocessed MLS V3 data to NRT MLS data in ERA5 at the beginning of 2015. However, we only use ERA5 data for years before 2003, and the good agreement seen between the CAMS reanalysis and ERA5 for the period 2003–2013 and between MSR, MOD, and ERA5 for the earlier years gives us confidence to extend our total column data set back in time to 1979 using ERA5 data.

Figure 1 illustrates that there is a large interannual variability in Arctic ozone in March, much of which is a result of changes in transport (both in the large-scale downward transport as well as meridional mixing with midlatitudes), and a downward trend to lower ozone columns in the Arctic during the 1990s (see also Figure 3.9 in WMO, 2018) owing to the higher concentrations of ozone depleting substances (Figures ES-1 and ES-2 in WMO, 2018). The figure also shows three years with exceptionally low Arctic ozone columns in March: 2020, 2011, and 1997. These three years will be compared in more detail in section 3.3. Low ozone columns are generally associated with a strong polar vortex, while high values are found when the polar vortex is weak or broken up (Newman et al., 1997). The lowest values in the time series are found in March 2020 with average TCO3 values north of 63°N in the CAMS reanalysis of 318 DU.

3. Arctic Stratospheric Ozone During the Winter 2019/2020

3.1. Climatological Means of TCO3, Temperatures, and Zonal Winds at 50 hPa

Figure 2 shows the climatological monthly mean fields from the CAMS reanalysis (averaged over the period 2003–2019) for TCO3, temperature (T) at 50 hPa, and zonal wind (U) at 50 hPa for the months December to April. The 50 hPa level was chosen because it is close to the maximum of the ozone layer, PSCs are formed close to this altitude, and hence, ozone depletion occurs around this level. The climatological TCO3 values (Figure 2a) increase from December to March with values above 450 DU in places in February and March. This springtime maximum is the result of descent in the Arctic stratosphere during the winter months and minimum photochemical loss during the polar night. The lowest temperatures at 50 hPa (Figure 2b) are usually found in December with values between −75°C and −80°C, illustrating that the climatological mean temperatures at 50 hPa in the Arctic during winter and spring are usually above the threshold for PSC formation (−78°C). The lowest temperatures are found north of Scandinavia with values increasing from December to April as sunlight returns to the polar regions. The low temperatures are an indication of the climatological position of the polar vortex and coincide with the lowest TCO3 values. The highest temperatures are found over Kamchatka and the Bering Sea. This coincides with the location of the highest ozone columns. During winter, the zonal winds are westerly in the stratosphere because of the large-scale meridional temperature gradient between the cold pole (no solar heating during the polar night) and the warmer midlatitudes. Figure 2c shows the belt of westerlies surrounding the North Pole that make up the polar vortex at this altitude, with the strongest zonal winds found in January and February. In an average year the polar vortex in the lower stratosphere usually forms in November, peaks in January, and dissipates in early April (Coy et al., 1997). Figure 2c confirms this, showing the weakening of the zonal winds at 50 hPa from February to April, as sunlight returns to high northern latitudes and the temperature

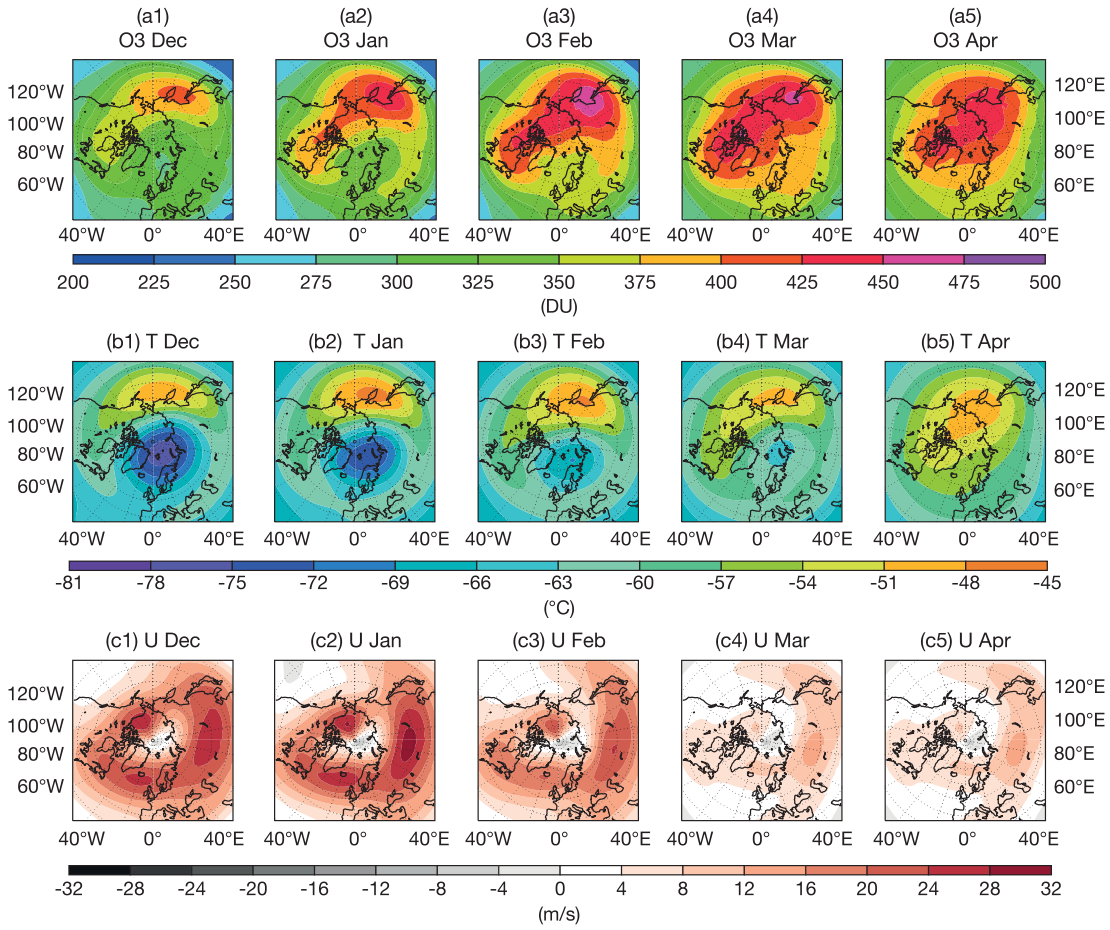

Figure 2. Climatological monthly means of (a) TCO3 (in DU), (b) temperature at 50 hPa (in °C), and (c) zonal wind (in m/s) from the CAMS reanalysis averaged over the years 2003–2019 for December (Column 1), January (Column 2), February (Column 3), March (Column 4), and April (Column 5).

contrast between the pole and the extratropics becomes weaker. The fact that the multiyear means of TCO3, T, and U are not symmetrical illustrates the impact that topography has on the circulation in the Arctic stratosphere.

3.2. Anomalies of TCO3, Temperatures, and Zonal Winds at 50 hPa in 2020

Figure 3 shows time series of Arctic minimum TCO3 and minimum temperatures at 50 hPa (both calculated for the area north of 60°N) from the CAMS reanalysis (2003–2020) and from ERA5 for the earlier years (1979–2002). The gray shading shows the range of the minimum values per day for the whole period 1979–2019 and the solid black line the mean values. The figure illustrates that minimum TCO3 values in the Arctic in late winter/spring show a large spread from year to year and lie between about 200 and 400 DU. Tegtmeier et al. (2008) showed that interannual variability in chemistry and the dynamical ozone supply due to transport processes (i.e., meridional mixing across vortex edge, mean transport by residual circulation, and diabatic descent in polar vortex) contribute equally to the variability of Arctic wintertime TCO3. The average minimum TCO3 values increase from January to April and lie above 250 DU the whole time. In 2020 (red line in Figure 3a) the situation is completely different. While minimum TCO3 values in January and February 2020 lie within the range of minimum values observed in other years, in March and April 2020 they are the lowest observed ozone columns in the whole record with the absolute minimum value of 211 on 18 March 2020. The previous two years with exceptionally low ozone values (2011 and 1997) are also shown in Figure 3 and will be discussed in more detail in section 3.3 below.

The time series of minimum temperatures at 50 hPa (Figure 3b) shows that the lowest temperatures are found during the winter months December and January and that on average temperatures increase from January onward as sunlight returns to the polar regions. We also see a large spread in mean minimum temperature

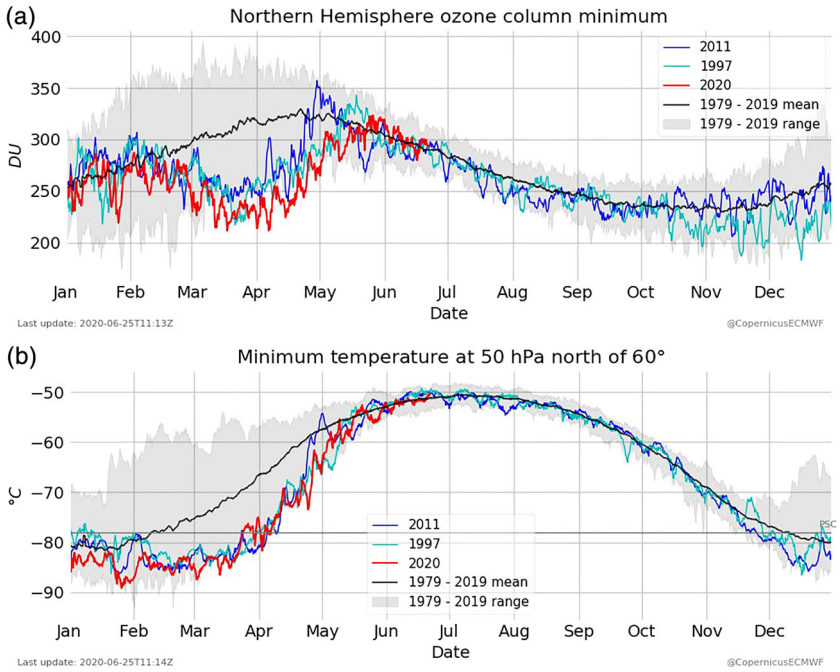

Figure 3. (a) Time series of minimum TCO3 (in DU) and (b) minimum temperature (in °C) at 50 hPa north of 60°N from CAMS reanalysis (covering the years 2003–2020) and ERA5 (1979–2002). The shaded gray area shows the range of minimum values per day over the entire period 1979–2019, the black curve the daily mean minimum values averaged over the period 1979–2019, the red curve the values for 2020, the blue curve the values for 2011, and the cyan curve the values for 1997.

values with some years having values no lower than −60°C while others have minimum temperatures below the PSC formation threshold of −78°C. This illustrates the large interannual variability in the Arctic stratosphere. The mean temperatures are just below the threshold for PSC formation for about 2 months from mid-December to early February but above it for the rest of winter and spring. Minimum temperatures in 2020 were some of the lowest in our record and below −78°C from the beginning of January until the last week of March. This was low enough for PSCs to form and suggests that the low Arctic ozone columns seen in 2020 are at least in part the result of in situ chemistry. In particular, the low temperatures in March, when more of the vortex is illuminated by the Sun, create a strong potential for catalytic ozone destruction. This will be discussed further in section 3.3 below.

Figure 4 shows the monthly mean anomalies of TCO3, T, and U at 50 hPa for December 2019 to April 2020 against the climatologies from the CAMS reanalysis (Figure 2). Anomalously low TCO3 values (Figure 4a) were found over the Arctic during January to April 2020 with the largest negative anomaly of more than −180 DU seen in March 2020, about 40% below the climatological values. The negative ozone anomaly lasted well into April when TCO3 values were still more than 140 DU (or 35%) below the climatology. These ozone anomalies were associated with the anomalously strong and long-lasting polar vortex illustrated by the stronger than average zonal winds at 50 hPa (Figure 4c) between January and April 2020, with the largest positive anomaly in March 2020. The polar vortex lasted well into April before it split into two around 19 April 2020. It was very stable and remained centered near the North Pole throughout, making it more akin to the polar vortex seen over Antarctic during winter/spring, and less like the more perturbed type usually found over the Arctic. The polar vortex was considerably colder than usual throughout the winter/spring of 2020 (Figure 4b). The largest temperature anomalies at 50 hPa were found in February and March 2020, when temperatures were more than 18°C and 21°C, respectively, below the climatological values. The low temperatures continued into April 2020 giving the potential for catalytic ozone depletion at a time when sunlight had returned to the Arctic region.

Newman et al. (2001) showed that the temperatures of the Arctic lower stratosphere in early March are driven by the strength and duration of planetary waves propagating into the stratosphere in middle to late winter. This can be illustrated by looking at the poleward eddy heat flux in middle to late winter, a key indicator

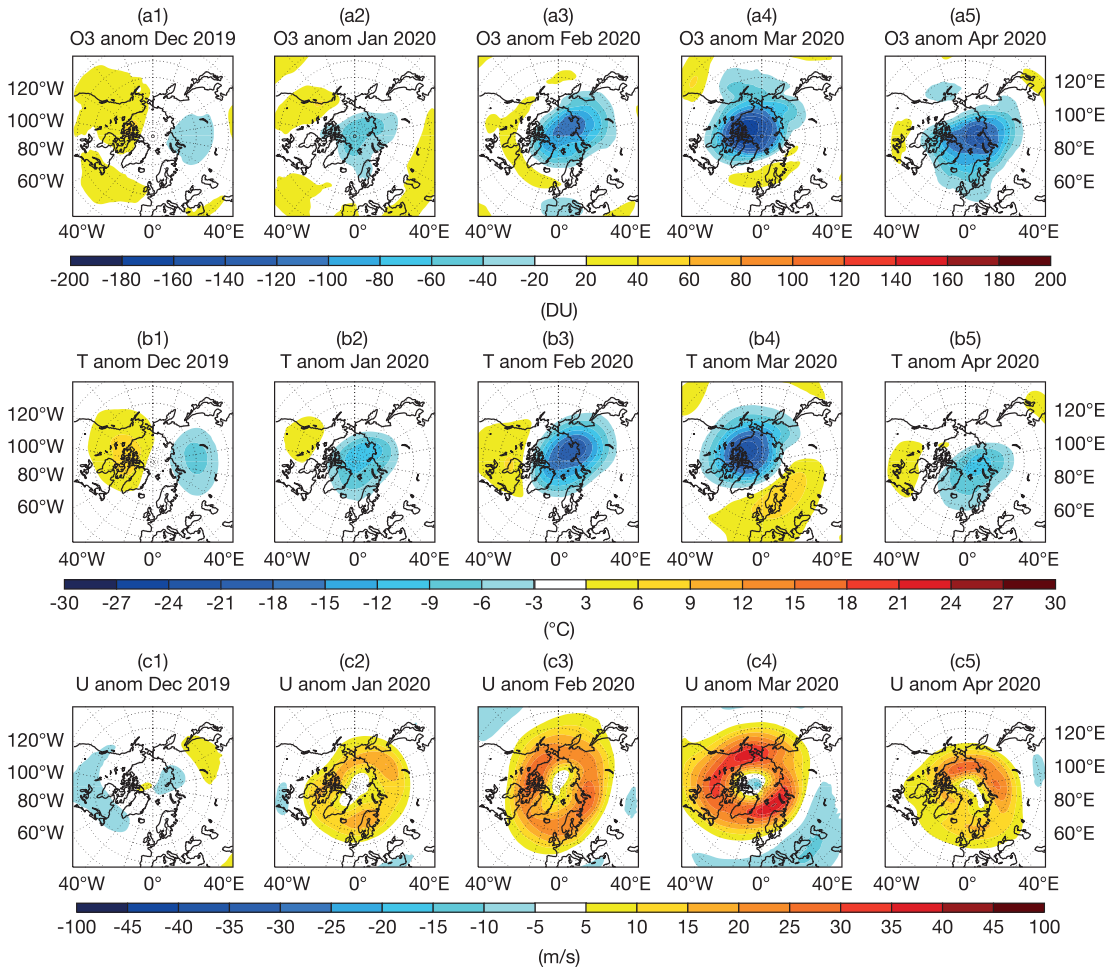

Figure 4. Monthly mean anomalies of (a) TCO3 (in DU), (b) temperature at 50 hPa (in °C), and (c) zonal wind (in m/s) from the CAMS reanalysis against the climatology calculated over the years 2003–2019 (see Figure 2) for December 2019 (Column 1), January 2020 (Column 2), February 2020 (Column 3), March 2020 (Column 4), and April 2020 (Column 5).

of the upward propagation of planetary waves, which is highly correlated with the mean polar stratospheric temperature during late winter. Low stratospheric temperatures are the result of weak wave forcing, and higher than average temperatures the result of strong wave forcing. Figure 5 shows the poleward 45-day running mean eddy heat flux at 50 hPa averaged between 45°N and 75°N from ERA5 for the winter/spring 2019/2020 compared to the years from 1979 onward. The years 1996/1997 and 2010/2011 are also shown and are discussed in section 3.3 below. It illustrates that spring 2020 was characterized by below average planetary wave driving between January and the end of March and that values between mid-February and mid-March were below the 10th percentile of the 1979–2019 period. This low wave driving led to the large cold temperature anomalies and exceptionally strong polar vortex seen in Figure 4.

The three-dimensional distribution of ozone in the stratosphere as well as the corresponding vertical ozone anomalies are shown in Figure 6. Figure 6a shows cross sections of climatological monthly mean ozone partial pressure values (2003–2019) from the surface to the upper stratosphere along one meridian (0°E/180°E) over the North Pole. They illustrate that the ozone layer is at higher altitudes in the tropics where maximum ozone partial pressure values are found around 20 hPa and at lower altitudes over the North Pole. Figure 6a also illustrates increased ozone maximum values in the lower stratosphere in the Arctic during February and March associated with the large-scale diabatic descent. The cross sections for the winter/spring months of 2020 (Figure 6b) are very different from the climatologies. In 2020, the ozone layer is considerably thinner than in the climatologies. Ozone values in the layer decrease and anomalies against the climatology (Figure 6c) increase from January to March, and values over the North Pole remain low in April 2020.

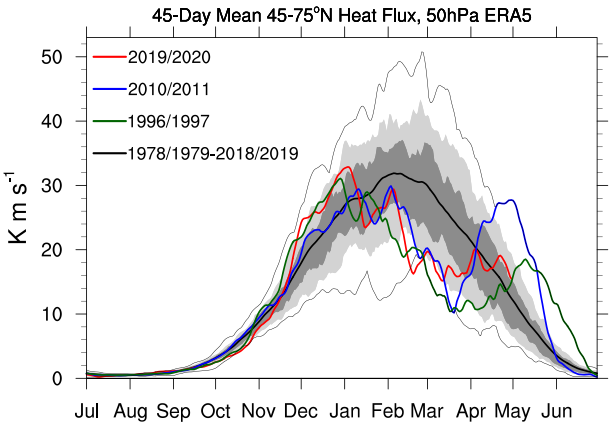

Figure 5. Eddy heat flux in km/s at 50 hPa averaged between 45°N and 75°N for the 45-day period prior to the date indicated, calculated from ERA5 data. The light shading is the 10th to 90th percentile and the darker shading the 75th–25th percentile. The thin black lines are maximum and minimum values, the thick black line the mean, the red line the values for winter/spring 2019/2020, the blue line for 2010/2011, and the green one for 1996/1997.

While some of the lower ozone values were the result of reduced meridional mixing and reduce diabatic downwelling during spring 2020 because of reduced wave activity as seen in low eddy heat fluxes at 50 hPa (Figure 5), there is the clear signature of chemical ozone depletion (see also Figure 13 below) leading to the extremely low ozone values over the North Pole in March and April 2020. In March 2020 ozone values in the ozone layer over the North pole are reduced to around 4 mPa in the monthly mean, more than 10 mPa below the climatological values. These low values last into April 2020. The anomaly plots for 2020 (Figure 6c) illustrate the vertical extent of the ozone anomalies during spring 2020, with the largest negative anomalies found over the Arctic during March and anomalies lasting into April. The chemical nature of the ozone loss in the Arctic during winter 2020 and the processes leading to it were documented in Manney et al. (2020) using MLS data. Wohltmann et al. (2020) calculated ozone loss in the winters of 2019/2020 and 2010/2011 by comparing a passive ozone tracer with ozonesonde profiles and found that minimum ozone mixing ratios at 450 K corresponded to a maximum chemical loss of about 2.8 ppm or 93% averaged over all sondes. Comparing the vortex mean from MLS and the passive ozone tracer run, they found a percentage ozone loss of 73% at 450 K in 2020 compared to 63% in 2011 with ozone loss peaking at lower altitudes in 2020 than 2011. These values are comparable to ozone loss typically found in the Antarctic ozone hole.

Figure 7 compares ozone and temperature profiles for January to April 2020 from ozonesondes at Ny-Ålesund with profiles from the CAMS reanalysis and against climatological ozone profiles. Ozonesondes are not assimilated in the CAMS reanalysis and therefore are completely independent validation data. The

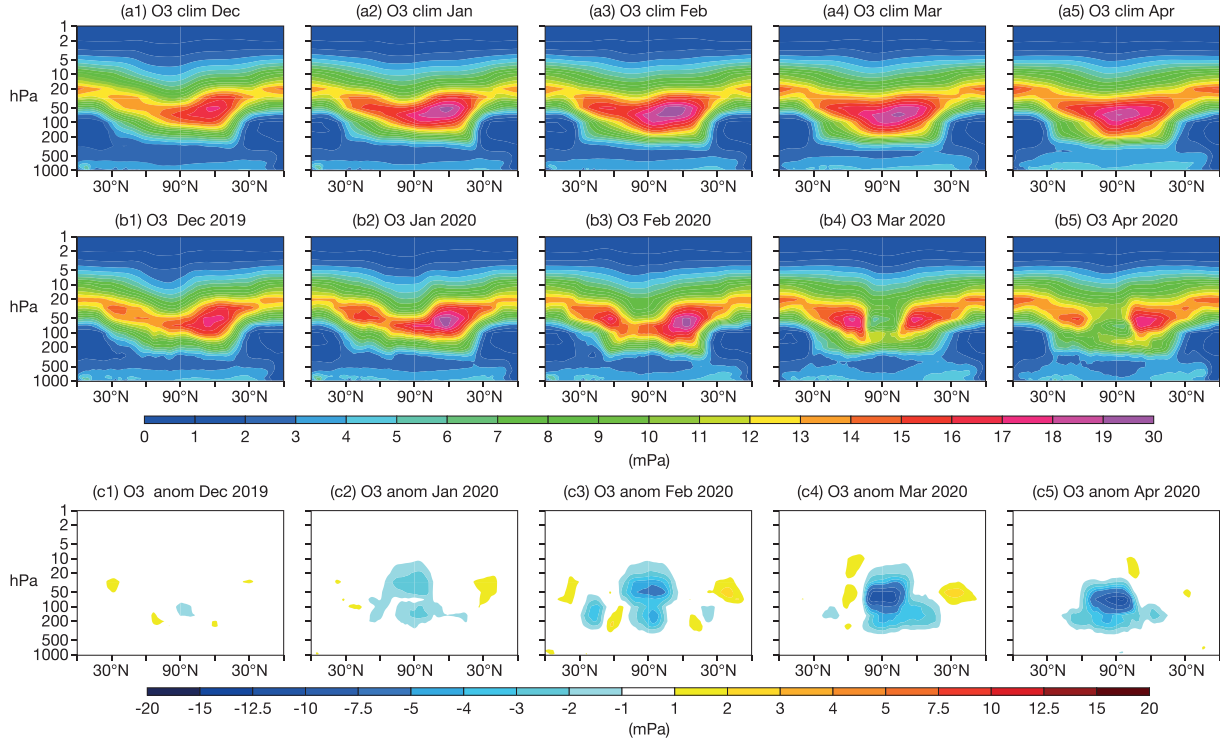

Figure 6. (a) Cross sections of monthly mean climatologically averaged ozone partial pressure (in mPa) from the CAMS reanalysis (2003–2019) along one meridian (0°E/180°E) from the equator north via the North Pole and back to the equator, (b) corresponding cross sections for 2019/2020, and (c) cross sections of anomalies for 2019/2020 for December (Column 1), January (Column 2), February (Column 3), March (Column 4), and April (Column 5).

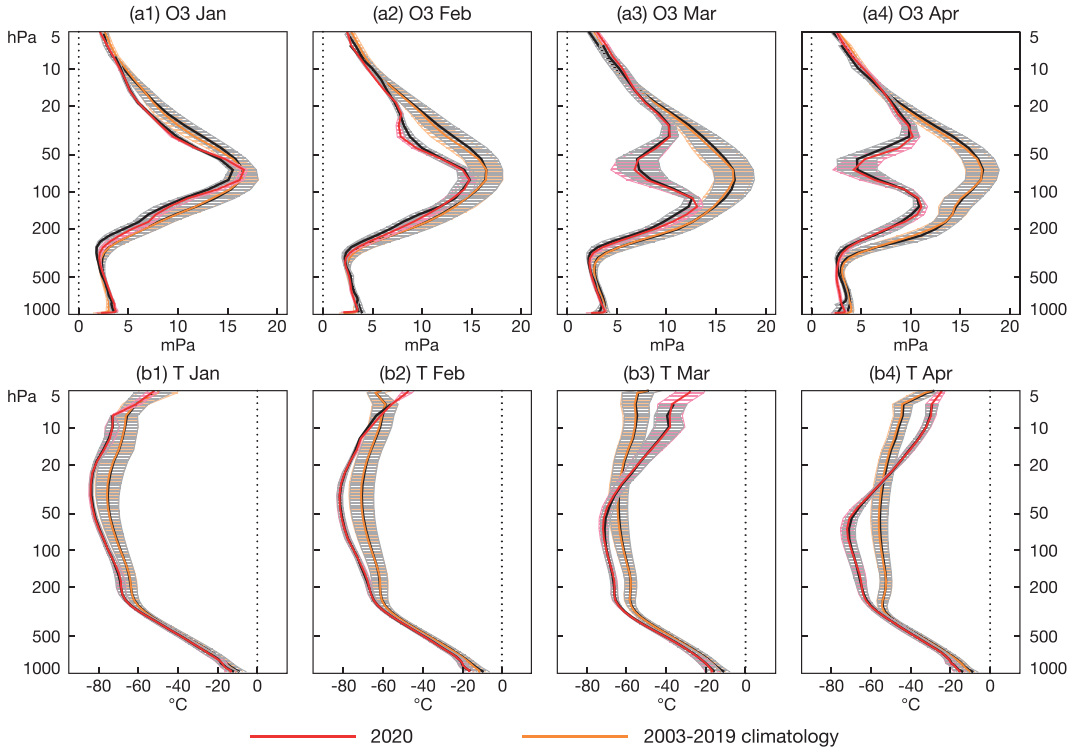

Figure 7. Comparisons of (a) ozone (in mPa) and (b) temperature (in °C) profiles from the CAMS reanalysis and ozonesondes at Ny-Ålesund for January (Column 1), February (Column 2), March (Column 3), and April (Column 4). The red profiles show monthly mean CAMS reanalysis values for 2020, and the orange profiles the climatological mean from the CAMS reanalysis (2003–2019). Black lines show the corresponding means from the ozonesondes. The hatched area depicts ±one standard deviation. The number of ozone profiles that went into the averages were January 2020: 6; February 2020: 8; March 2020: 16; April 2020: 13; January climatology: 187; February climatology: 178; March climatology: 177; and April climatology: 98.

climatological monthly ozone profiles at Ny-Ålesund show the increase of ozone values in the lower stratosphere due to the large-scale diabatic descent between January and April with a thicker ozone layer and increased partial pressure values between 50 and 200 hPa. The climatological monthly means calculated from the CAMS reanalysis agree very well with sonde averages. Figure 7a shows that in 2020 the monthly mean ozone values are lower than the climatological values in all 4 months with a thinner ozone layer in January and February 2020, which must be the result of reduced large-scale transport and associated downwelling in 2020. This is followed by a clear indication of ozone depletion in March 2020 and April 2020, when the 2020 monthly mean values are below 5 mPa between 50 and 70 hPa. Such ozone profiles are very unusual for the Arctic in boreal spring and much more akin to ozone profiles found over the Antarctic during the SH ozone hole season in October. The temperature profiles (Figure 7b) show that 2020 is considerably colder than the CAMS climatology between 30 and 200 hPa throughout the period, with monthly mean temperatures below −78°C in January–March. Figure 8 shows four individual ozone profiles at Ny-Ålesund from the CAMS reanalysis and sondes and illustrates that in the last week of March 2020 ozone was almost completely depleted in a layer between 50 and 80 hPa, with partial pressures below 2 mPa. This layer of low ozone values remained visible in ozonesonde profiles at Ny-Ålesund until 15 April 2020 (see also Figure 11 below), while the subsequent ascent on 22 April 2020 had values between 10 and 18 mPa all the way between 20 and 200 hPa, indicating the end of the 2020 Arctic "ozone hole" at Ny-Ålesund.

3.3. Comparison of Arctic Ozone in Spring 2020 With 2011 and 1997

The time series of average TCO3 north or 63°N in Figure 1 shows how exceptionally low ozone columns over the Arctic were during March 2020 with averaged Arctic values down to 318 DU. Only two other years in the time series have had similarly low Arctic mean ozone values in March since 1979: 2011 with 327 DU and 1997 with 321 DU. In all three years, it was the unusual meteorological situation with a long-lasting and

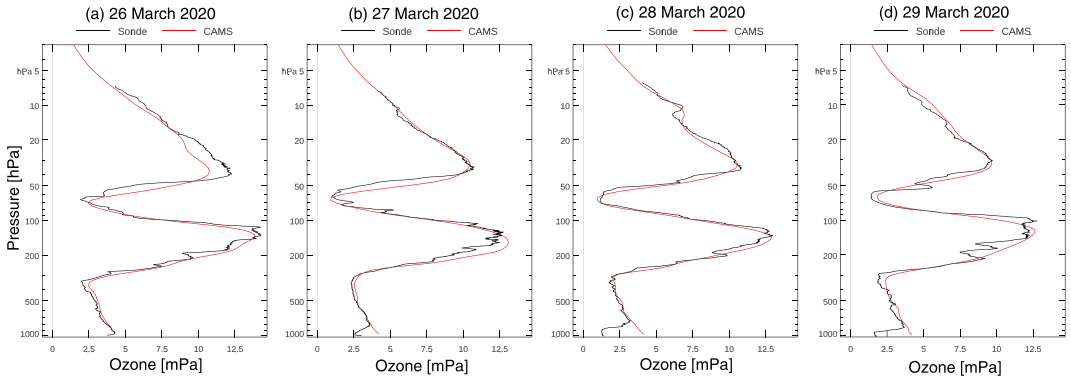

Figure 8. Ozone profiles in mPa from CAMS reanalysis (red) and ozonesondes (black) at Ny-Ålesund on (a) 26, (b) 27, (c) 28, and (d) 29 March 2020.

cold polar vortex centered over the North Pole (Coy et al., 1997; Manney et al., 2011) that led to exceptional ozone losses. All three years were characterized by weak planetary wave driving from the troposphere (Hurwitz et al., 2011; Newman et al., 2001; Shaw & Perlwitz, 2014). This is illustrated by the mean eddy heat fluxes at 50 hPa (Figure 5) which were below average in all three years from January to the end of March and below the 10th percentile of the period 1979–2019 from mid-February to March. The lowest values where generally seen in 1997 from late January to April, apart from a brief period in February when values were lower in 2020. This low wave driving led to large cold temperature anomalies and exceptionally strong polar vortex in all three years. The time series in Figure 3a shows the daily TCO3 minimum values for 2020, 2011, and 1997 and illustrates that from late January until the end of April the minimum values in 2020 were lower than in 2011 and 1997. The lowest TCO3 minimum value in 2020 was 211 DU (on 18 March), compared to 232 DU in 2011 (on 26 February) and 217 DU in 1997 (on 21 March). The time series of the minimum temperatures at 50 hPa north of 60°N (Figure 3b) shows that in 1997 temperatures were around average until early February and then fell in February. Temperatures in the first half of January 2011 were also around or above average, but in 2020 temperatures in the lower stratosphere were below average from the beginning of January and remained below the PSC formation threshold of −78°C until the last week of March.

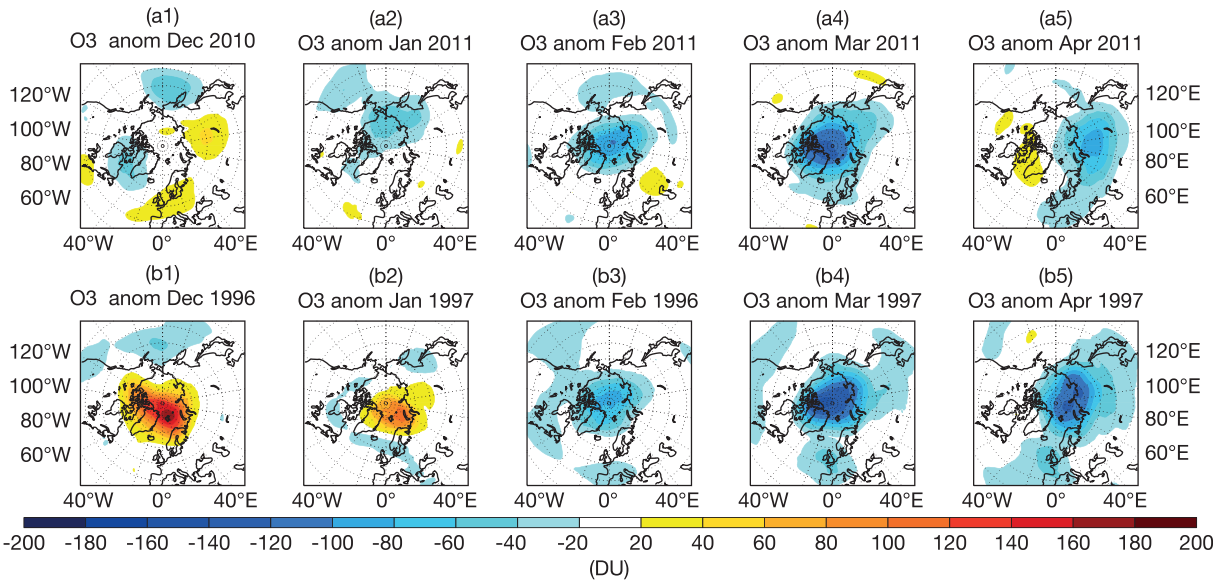

Figure 9. Monthly mean anomalies of TCO3 in DU from (a) the CAMS reanalysis for 2010/2011 and (b) ERA 5 1996/1997 against climatologies calculated over the years 2003–2019 (see Figure 2) for December (Column 1), January (Column 2), February (Column 3), March (Column 4), and April (Column 5).

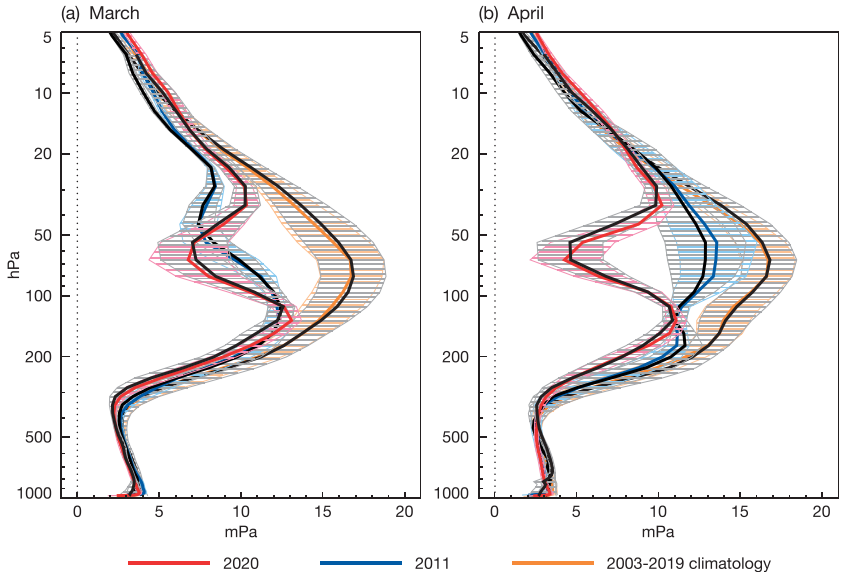

Figure 10. Monthly mean ozone profiles in mPa at Ny-Ålesund for (a) March and (b) April. The red profiles show the 2020 monthly means, the blue profiles the 2011 monthly means, and the orange profiles the climatological means from the CAMS reanalysis (2003–2019). Black lines show the corresponding means from the ozonesondes. The hatched areas depict ±one standard deviation. The number of ozone profiles that went into the averages are March 2020: 16; March 2011: 17; March climatology: 177; April 2020: 13; April 2011: 10; and April climatology: 98.

Figure 9 shows the monthly TCO3 anomalies for the winters 1996/1997 and 2010/2011 against the CAMS climatology (using the same reference period 2003–2019). The corresponding anomalies for 2019/2020 can be found in Figure 4. All three winters had a long-lasting, cold polar vortex centered over the North Pole. However, in 1996/1997 the polar vortex did not form until late December and was weaker than normal with above average temperatures until the end of January (Coy et al., 1997). The vortex was then strong and centered around the North Pole until it broke up in late April. As a result, we see positive TCO3 anomalies in December 1996 and January 1997 (Figure 9b), while in January 2020 and 2011 (Figure 9a) negative TCO3 anomalies can already be seen over the North Pole. In February–April large negative TCO3 anomalies are found in all three winters (see also Figure 4) with the largest overall anomalies found in 2020 when values were about 27% (February), 40% (March), and 35% (April) below the CAMS climatology. This compares with anomalies of −25% (February 2011), −31% (March 2011), and −22% (April 2011) and −22% (February 1997), −35% (March 1997), and −30% (April 1997) in the other two years.

In Figure 10 we compare ozone profiles at Ny-Ålesund from sondes and the CAMS reanalysis for March and April 2020 and 2011 with the CAMS climatology. The CAMS data were interpolated to the times and location of the sondes. The figure shows that in 2020 the exceptionally low ozone values in the lower stratosphere lasted into April, while in 2011 values had already increased again in April. Figure 11 shows time series of ozone profiles at Ny-Ålesund from sondes and the CAMS reanalysis for 2020 and 2011. Figure 11 shows clearly very low ozone partial pressure values in 2020 between mid-March and mid-April in the altitude range of 50–80 hPa. In 2011 low ozone partial pressure values were also seen throughout March, located at slightly higher altitude, but minimum values were not as low as in 2020. The period of very low ozone values ended at the end of March 2011 and by 4 April 2011 ozone profiles at Ny-Ålesund had values over 10 mPa everywhere between 30 and 200 hPa. However, this recovery did not happen until much later in 2020. An ascent at Ny-Ålesund on 15 April 2020 still showed ozone partial pressures down to 2 mPa between 60 and 70 hPa, and only the subsequent ascent on 22 April 2020 did not show the low values any more. In both years the polar vortex was long lasting and was centered around the pole so that profiles at Ny-Ålesund are adequate to illustrate the differences between the years. Figure 12 shows the vortex-averaged ozone daily mean mixing ratios on the 475 K isentropic surface (about 19 km) for 2020 and 2011. The 36 PVU (potential vorticity unit) contour was used to determine the edge of the polar vortex following Rex et al. (1999). The vortex average ozone mixing ratios at 475 K were lower in 2020 than in 2011. Both years

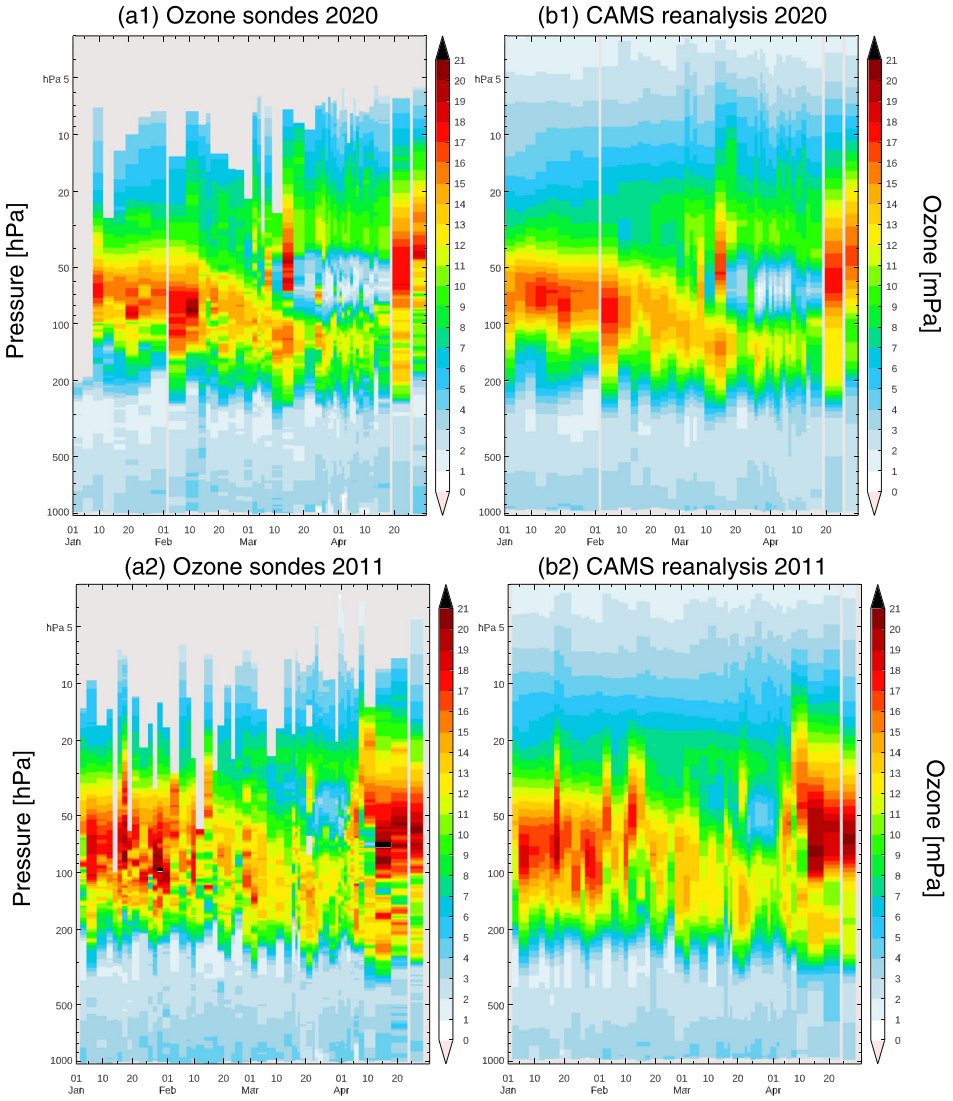

Figure 11. Time series from January to April of ozone profiles (in mPa) at Ny-Ålesund from ozonesondes (a) and the CAMS reanalysis (b) for 2020 (Row 1) and 2011 (Row 2).

show the lowest vortex-averaged ozone mixing ratios in the second half of March and early April, with mean values lower in 2020 than in 2011 and down to below 1.5 ppmv in both years.

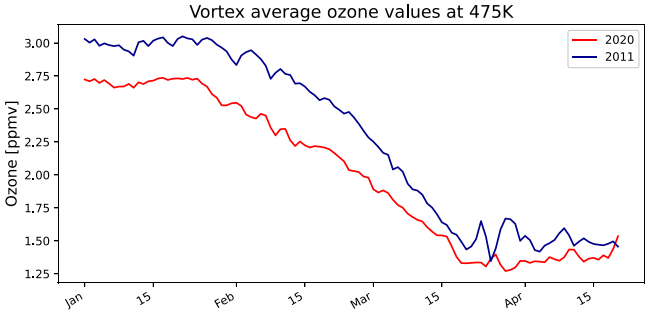

Figure 12. Vortex average daily mean ozone mixing ratios in ppmv on the 475 K isentropic surface for 2020 (red) and 2011 (blue). The 36 PVU (potential vorticity unit) value was chosen to define the edge of the polar vortex.

Evidence that the exceptionally low ozone values seen in 2020 (and 2011) were the result of chemical ozone depletion comes from the ACE-FTS (Sheese et al., 2017) and MLS (Livesey et al., 2018) profiles (Figure 13). Monthly mean ASC-FTS and MLS profiles averaged over the latitude band 60–90°N show reduced concentrations of the chlorine reservoir species hydrochloric acid (HCl) and exceptionally high abundances of chlorine monoxide (ClO) during March 2020 and 2011 relative to the ACE-FTS or MLS climatologies. The maximum of ClO is found at lower altitude in 2020 than 2011, which was also seen by Manney et al. (2020). There are signs of denitrification in both years with reduced concentrations of nitric acid (HNO_3). This is evidence that PSCs formed during spring 2020 (and 2011), chlorine activation happened and catalytic ozone depletion led to the very low ozone values seen during March 2020 (and 2011). Overall MLS and

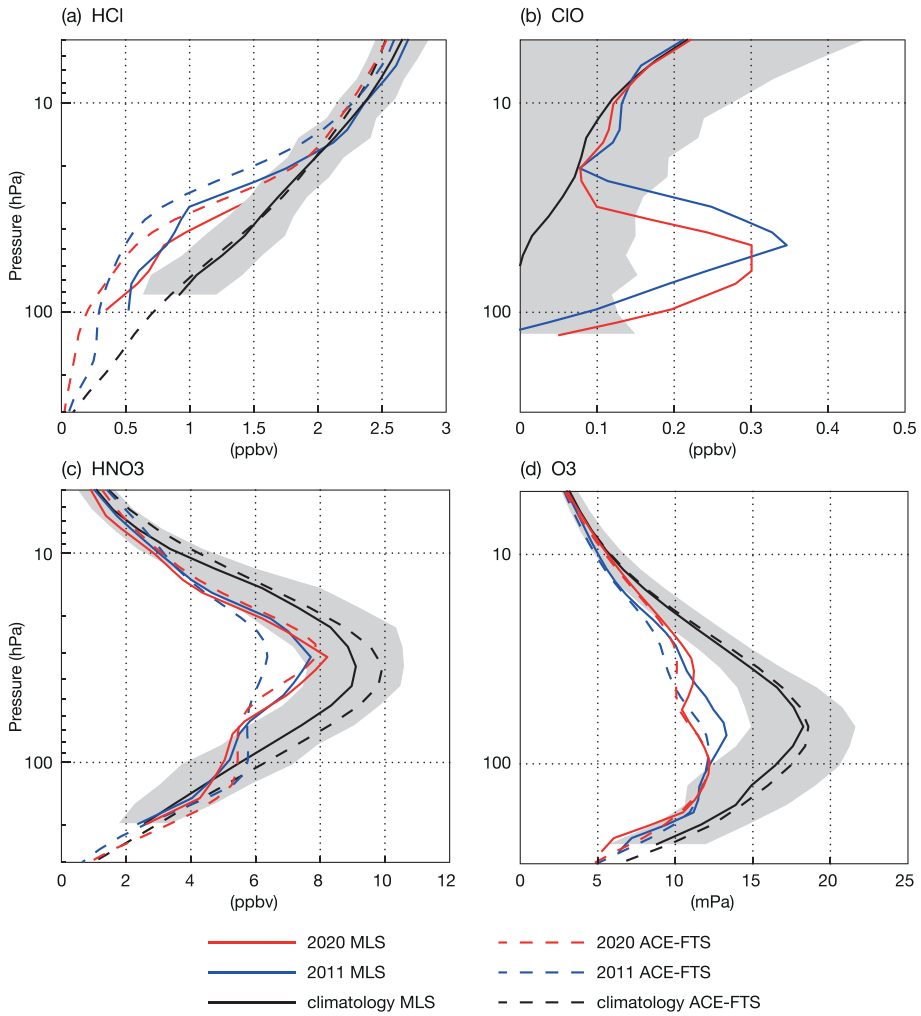

Figure 13. (a) HCl, (b) ClO, (c) HNO_3, and (d) ozone mean vertical profiles for March from MLS v4.2 retrievals (solid lines) and ACE-FTS v3.6 retrievals (dashed lines) poleward of 60°N. Shown are 2005–2019 climatologies excluding 2011 (black lines), March 2011 (blue line) and March 2020 (red lines). The gray envelopes represent two standard deviations of all profiles in each MLS climatology. All retrievals are expressed in volume mixing ratios (ppbv) except for ozone which is in partial pressure (mPa).

ACE-FTS agree very well, despite the much sparser sampling of ACE-FTS. The only exception is HNO_3 where ACE-FTS indicates more HNO_3 depletion in 2011 than in 2020 while MLS shows nearly the same abundances. This apparent disagreement is due to the more limited sampling in ACE-FTS; that is, during the first half of March 2011 ACE-FTS happened to sample latitudes with very strong HNO_3 depletion while MLS sampled more locations. The sampling of data inside or outside the polar vortex might also explain some of the discrepancy seen in HNO_3 between MLS and ACE-FTS.

4. Conclusions

Data from a reanalysis of atmospheric composition produced by the Copernicus Atmosphere Monitoring Service, the so-called CAMS reanalysis, augmented by ERA5 data for years prior to 2003 were used to assess stratospheric Arctic ozone during the winter and spring of 2019/2020 and to compare it with other years since 1979. During winter and spring 2020, the Arctic polar vortex was exceptionally strong, long-lived, cold, and remained centered around the North Pole until the second half of April. This was the result of weak planetary-scale wave forcing during middle to late winter. For several months, minimum temperatures in the Arctic lower stratosphere were low enough to allow the formation of PSCs, and ozone columns over

large parts of the Arctic reached record low values in March and April 2020. Minimum total column ozone values were below 250 DU for most of March and the first half of April with the lowest values of 211 DU found on 18 March 2020 in the CAMS reanalysis. Such low ozone columns are extremely unusual for the NH winter/spring. They were even lower than during the previously recorded cases of large Arctic ozone depletion in 2011 and 1997 when the CAMS/ERA5 data set had minimum values of 232 and 217 DU, respectively. Monthly mean Arctic TCO3 values in March 2020 were up to 180 DU or 40% lower than the CAMS climatology (calculated over the period 2003–2019) while values for 2011 and 1997 were up to 31% and 35% lower, respectively.

While some of the lower ozone values were the result of reduced diabatic downwelling and reduced meridional transport during spring 2020 because of reduced tropospheric planetary wave activity, there is evidence that chemical ozone destruction occurred and led to extremely low values in the ozone layer over the North Pole in March and April 2020. Profiles from MLS and ACE-FTS show large increases in ClO and reductions in the concentrations of HNO_3 and HCl in March 2020, consistent with the presence of PSCs. Ozone profiles from sondes and the CAMS reanalysis at Ny-Ålesund show that ozone was severely depleted in a layer between 80 and 50 hPa where ozone partial pressure values below 2 mPa were observed at the end of March 2020. The layer of severely depleted ozone concentrations lasted until the middle of April 2020 as seen in CAMS ozone profiles and ozonesondes, longer than in 2011 when low ozone values ceased at the end of March.

The CAMS reanalysis was able to capture the exceptional Arctic ozone hole of 2020 well with good agreement between CAMS ozone profiles and independent ozonesonde data. Studies are ongoing to determine why tropospheric planetary wave forcing was so weak in winter/spring 2020 and if there was any feedback from the Arctic ozone depletion onto the dynamics that helped to prolong the strong vortex. An interesting question would also be to investigate whether and to what extent ash and SO_2 that were injected into the Arctic stratosphere after the Raikoke eruption in June 2019 helped to enhance PSC formation and the subsequent ozone depletion in the Arctic during spring 2020. It remains to be seen if this kind of Arctic ozone hole will continue to be an exceptional event or occur more often in a changing climate.

Data Availability Statement

CAMS reanalysis data are freely available from the CAMS Atmosphere Data Store (ADS, https://ads.atmosphere.copernicus.eu/cdsapp#!/home), and ERA5 data are available from the Climate Data Store (CDS, https://cds.climate.copernicus.eu/#!/home). The MSR data were downloaded from the Temis website (http://www.temis.nl), and NASA's MOD data are available online (at https://acd-ext.gsfc.nasa.gov/Data_services/merged/). The ozonesondes at Ny-Ålesund were launched by the Alfred-Wegener-Institut Helmholtz-Zentrum für Polar- und Meeresforschung (AWI) and obtained from NDACC (see http://www.ndacc.org).

Acknowledgments

The Copernicus Atmosphere Monitoring Service is operated by the European Centre for Medium-Range Weather Forecasts on behalf of the European Commission as part of the Copernicus program (http://copernicus.eu). Thanks to Luke Jones for providing the tools for the validation against ozonesondes and to Anabel Bowen for improving some of the figures. Thanks to the data providers of the data assimilated in the CAMS reanalysis and the data used for the validation studies in this paper. ACE-FTS (http://www.ace.uwaterloo.ca/data.php) is an instrument of the Canadian-led Atmospheric Chemistry Experiment (also known as SCISAT) that is mainly supported by the CSA and NSERC. We acknowledge the MLS (https://mls.jpl.nasa.gov/data/overview.php) mission scientists and associated NASA personnel for the production of the data used in this study.

References

Brewer, A. W. (1949). Evidence for a world circulation provided by measurements of helium and water vapour distribution in the stratosphere. *Quarterly Journal of the Royal Meteorological Society*, *75*, 351. https://doi.org/10.1002/qj.49707532603

Cariolle, D., & Déqué, M. (1986). Southern Hemisphere medium-scale waves and total ozone disturbances in a spectral general circulation model. *Journal of Geophysical Research*, *91*, 10,825–10,846.

Cariolle, D., & Teyssèdre, H. (2007). A revised linear ozone photochemistry parameterization for use in transport and general circulation models: Multi-annual simulations. *Atmospheric Chemistry and Physics*, *7*, 2183–2196. https://doi.org/10.5194/acp-7-2183-2007

Courtier, P., Thépaut, J.-N., & Hollingsworth, A. (1994). A strategy for operational implementation of 4D-Var, using an incremental approach. *Quarterly Journal of the Royal Meteorological Society*, *120*, 1367–1388.

Coy, L., Newman, P. A., & Nash, E. R. (1997). Meteorology of the polar vortex: March 1997. *Geophysical Research Letters*, *24*(22), 2693–2696.

Dobson, G. M. G. (1956). Origin and distribution of polyatomic molecules in the atmosphere. *Proceedings of the Royal Society of London A*, *236*, 187–193.

Dragani, R. (2011). On the quality of the ERA-interim ozone reanalyses:Comparisons with satellite data. *Quarterly Journal of the Royal Meteorological Society*, *137*, 1312–1326. https://doi.org/10.1002/qj.82110.1002/qj.821

Flemming, J., Benedetti, A., Inness, A., Engelen, R. J., Jones, L., Huijnen, V., et al. (2017). The CAMS interim reanalysis of carbon monoxide, ozone and aerosol for 2003–2015. *Atmospheric Chemistry and Physics*, *17*, 1945–1983. https://doi.org/10.5194/acp-17-1945-2017

Flemming, J., Huijnen, V., Arteta, J., Bechtold, P., Beljaars, A., Blechschmidt, A.-M., et al. (2015). Tropospheric chemistry in the integrated forecasting system of ECMWF. *Geoscientific Model Development*, *8*, 975–1003. https://doi.org/10.5194/gmd-8-975-2015

Flemming, J., Inness, A., Jones, L., Eskes, H. J., Huijnen, V., Schultz, M. G., et al. (2011). Forecasts and assimilation experiments of the Antarctic ozone hole 2008. *Atmospheric Chemistry and Physics*, *11*, 1961–1977. https://doi.org/10.5194/acp-11-1961-2011

Garcia, R. R., & Boville, B. A. (1994). "Downward control" of the mean meridional circulation and temperature distribution of the polar winter stratosphere. *Journal of the Atmospheric Sciences*, *51*, 2238–2245. https://doi.org/10.1175/1520-0469(1994)051<2238:COTMMC>2.0.CO;2

Groß, J.-U., & Müller, R. (2020). Simulation of the record Arctic stratospheric ozone depletion in 2020, submitted to J. Geophys. Res., https://doi.org/10.1002/essoar.10503569.1

Hersbach, H., Bell, B., Berrisford, P., Hirahara, S., Horanyi, A., Munoz-Sabater, J., et al. (2020). The ERA5 global reanalysis. *Quarterly Journal of the Royal Meteorological Society*, *146*, 1999–2049. https://doi.org/10.1002/qj.3803

Huijnen, V., Miyazaki, K., Flemming, J., Inness, A., Sekiya, T., & Schultz, M. G. (2020). An intercomparison of tropospheric ozone reanalysis products from CAMS, CAMS interim, TCR-1, and TCR-2. *Geoscientific Model Development*, *13*, 1513–1544. https://doi.org/10.5194/gmd-13-1513-2020

Huijnen, V., Williams, J., van Weele, M., van Noije, T., Krol, M., Dentener, F., et al. (2010). The global chemistry transport model TM5: Description and evaluation of the tropospheric chemistry Version 3.0. *Geoscientific Model Development*, *3*, 445–473. https://doi.org/10.5194/gmd-3-445-2010

Hurwitz, M. M., Newman, P. A., & Garfinkel, C. I. (2011). The Arctic vortex in March 2011: Adynamical perspective. *Atmospheric Chemistry and Physics*, *11*(22), 11,447–11,453.

Inness, A., Ades, M., Agustí-Panareda, A., Barré, J., Benedictow, A., Blechschmidt, A.-M., et al. (2019). The CAMS reanalysis of atmospheric composition. *Atmospheric Chemistry and Physics*, *19*, 3515–3556. https://doi.org/10.5194/acp-19-3515-2019

Inness, A., Baier, F., Benedetti, A., Bouarar, I., Chabrillat, S., Clark, H., et al. (2013). The MACC reanalysis: An 8 yr data set of atmospheric composition. *Atmospheric Chemistry and Physics*, *13*, 4073–4109. https://doi.org/10.5194/acp-13-4073-2013

Inness, A., Blechschmidt, A.-M., Bouarar, I., Chabrillat, S., Crepulja, M., Engelen, R. J., et al. (2015). Data assimilation of satellite-retrieved ozone, carbon monoxide and nitrogen dioxide with ECMWF's composition-IFS. *Atmospheric Chemistry and Physics*, *15*, 5275–5303. https://doi.org/10.5194/acp-15-5275-2015

Laeng, A., von Clarmann, T., Stiller, G., Grabowski, U., Kiefer, M., Hubert, D., et al. (2018). The ozone climate change initiative: Comparison of four Level-2 processors for the Michelson Interferometer for Passive Atmospheric Sounding (MIPAS). *Remote Sensing of Environment*, *162*, 316–343. https://doi.org/10.1016/j.rse.2014.12.013

Lawrence, A. D., Perlwitz, J., Butler, A. H., Manney, G. L., Newman, P. A., Lee, S. H., & Nash, E. R. (2020). The remarkably strong Arctic stratospheric polar vortex of winter 2020: Links to record-breaking Arctic oscillation and ozone loss, Submitted to. *Journal of Geophysical Research: Atmosphere*, *125*, e2020JD033271. https://doi.org/10.1002/essoar.10503356, https://doi.org/10.1029/2020JD033271

Lefever, K., van der A, R., Baier, F., Christophe, Y., Errera, Q., Eskes, H., et al. (2015). Copernicus stratospheric ozone service, 2009–2012: Validation, system intercomparison and roles of input data sets. *Atmospheric Chemistry and Physics*, *15*, 2269–2293. https://doi.org/10.5194/acp-15-2269-2015

Livesey, N J., Read, William G., Wagner, P. A., Froidevaux, L., Lambert, A., Manney, G. L., et al. (2018). Version 4.2x Level 2 data quality and description document, Tech. rep., Jet Propulsion Laboratory. Retrieved from https://mls.jpl.nasa.gov/data/v4-2_data_quality_document.pdf

Manney, G., Santee, M., Rex, M., Livesey, N. J., Pitts, M. C., Veefkind, P., et al. (2011). Unprecedented Arctic ozone loss in 2011. *Nature*, *478*(7370), 469–475. https://doi.org/10.1038/nature10556

Manney, G., Zurek, R. W., O'Neill, A., & Swinbank, R. (1994). On the motion of air through the stratospheric polar vortex. *Journal of the Atmospheric Sciences*, *51*, 2973–2994. https://doi.org/10.1175/1520-0469(1994)051<2973:OTMOAT>2.0.CO;2

Manney, G. L., Livesey, N. J., Santee, M. L., Froidevaux, L., Lambert, A., Lawrence, Z. D., et al. (2020). Record-low Arctic stratospheric ozone in 2020: MLS observations of chemical processes and comparisons with previous extreme winters. *Geophysical Research Letters*, *47*, e2020GL089063. https://doi.org/10.1029/2020GL089063

Newman, P. A., Gleason, J. F., & Stolarski, R. S. (1997). Anomalously low ozone over the Arctic. *Geophysical Research Letters*, *24*(22), 2689–2692.

Newman, P. A., Nash, E. R., & Rosenfield, J. E. (2001). What controls the temperature in the Arctic stratosphere in the spring? *Journal of Geophysical Research*, *106*(D17), 19,999–20,010.

Rex, M., von Der Gathen, P., Braathen, G., Harris, N., Reimer, E., Beck, A., & Zerefos, C. (1999). Chemical ozone loss in the Arctic winter 1994/95 as determined by the Match technique. *Journal of the Atmospheric Sciences*, *32*, 35–59. https://doi.org/10.1023/A:1006093826861

Salawitch, R. J. (Lead Author), Fahey, D. W., Hegglin, M. I., McBride, L. A., Tribett, W. R., & Doherty, S. J. (2019). Twenty questions and answers about the ozone layer: 2018 update, Scientific Assessment of Ozone Depletion: 2018, p. 84, World Meteorological Organization, Geneva, Switzerland.

Shaw, T. A., & Perlwitz, J. (2014). On the Control of the Residual Circulation and Stratospheric Temperatures in the Arctic by Planetary Wave Coupling. *Journal of the Atmospheric Sciences*, *71*, 195–206. https://doi.org/10.1175/JAS-D-13-0138.1

Sheese, P. E., Walker, K. A., Boone, C. D., Bernath, P. F., Froidevaux, L., Funke, B., et al. (2017). ACE-FTS ozone, water vapour, nitrous oxide, nitric acid, and carbon monoxide profile comparisons with MIPAS and MLS. *Journal of Quantitative Spectroscopy and Radiative Transfer*, *186*, 63–80. https://doi.org/10.1016/j.jqsrt.2016.06.026

Shepherd, T. G. (2008). Dynamics, stratospheric ozone, and climate change. *Atmosphere-Ocean*, *46*(1), 117–138. https://doi.org/10.3137/ao.460106

Stolarski, R. S., & Frith, S. M. (2006). Search for evidence of trend slow-down in the long-term TOMS/SBUV total ozone data record: The importance of instrument drift uncertainty. *Atmospheric Chemistry and Physics*, *6*, 4057–4065. https://doi.org/10.5194/acp-6-4057-2006

Tegtmeier, S., Rex, M., Wohltmann, I., & Krüger, K. (2008). Relative importance of dynamical and chemical contributions to Arctic wintertime ozone. *Geophysical Research Letters*, *35*, L17801. https://doi.org/10.1029/2008GL034250

van der A, R. J., Allaart, M. A. F., & Eskes, H. J. (2015). Extended and refined multi sensor reanalysis of total ozone for the period 1970–2012. *Atmospheric Measurement Techniques*, *8*, 3021–3035. https://doi.org/10.5194/amt-8-3021-2015

Waugh, D. W., Sobel, A., & Polvani, L. M. (2017). What is the Polar Vortex and how does it influence weather? *Bulletin of the American Meteorological Society*, *98*, 37–44. https://doi.org/10.1175/BAMS-D-15-00212.1

WMO (World Meteorological Organization), Scientific Assessment of Ozone Depletion (2018). Global ozone research and monitoring project (Report No. 58, p. 588). Geneva, Switzerland. Geneva, Switzerland.

Wohltmann, I., von der Gathen, P., Lehmann, R., Maturilli, M., Deckelmann, H., Manney, G. L., et al. (2020). Near complete local reduction of Arctic stratospheric ozone by severe chemical loss in spring 2020. *Geophysical Research Letters*, *47*, e2020GL089547. https://doi.org/10.1002/essoar.10503518.1

Yarwood, G., Rao, S., Yocke, M., & Whitten, G. (2005). Updates to the carbon bond chemical mechanism: CB05, Final report to the US EPA (EPA Report Number: RT-0400675). Retrieved from http://www.camx.com

References From the Supporting Information

Hubert, D., Lambert, J.-C., Verhoelst, T., Granville, J., Keppens, A., Baray, J.-L., et al. (2016). Ground-based assessment of the bias and long-term stability of 14 limb and occultation ozone profile data records. *Atmospheric Measurement Techniques*, *9*(6), 2497–2534. https://doi.org/10.5194/amt-9-2497-2016

Komhyr, W. D., Barnes, R. A., Borthers, G. B., Lathrop, J. A., Kerr, J. B., & Opperman, D. P. (1995). Electrochemical concentration cell ozonesonde performance evaluation during STOIC 1989. *Journal of Geophysical Research*, *100*, 9231–9244.

Langerock, B., de Mazière, M., Hendrick, F., Vigouroux, C., Desmet, F., Dils, B., & Niemeijer, S. (2015). Description of algorithms for co-locating and comparing gridded model data with remote-sensing observations. *Geoscientific Model Development*, *8*, 911–921. https://doi.org/10.5194/gmd-8-911-2015

Stauffer, R. M., Thompson, A. M., Kollonige, D. E., Witte, J. C., Tarasick, D. W., Davies, J., et al. (2020). A post-2013 dropoff in total ozone at a third of global ozonesonde stations: Electrochemical concentration cell instrument artifacts? *Geophysical Research Letters*, *47*, e2019GL086791. https://doi.org/10.1029/2019GL086791